# Supplementary information for "Electroresponsive structuring and friction of a non-halogenated ionic liquid in a polar solvent: Effect of concentration"

Georgia A. Pilkington[a,*], Anna Oleshkevych[a], Patricia Pedraz[a], Seiya Watanabe[a,†], Milad Radiom[a], Akepati Bhaskar Reddy[b], Alexei Vorobiev[c], Sergei Glavatskih[b,d], and Mark W. Rutland[a,e]

*[a]Division of Surface and Corrosion Science, School of Engineering Sciences in Chemistry, Biotechnology and Health, KTH Royal Institute of Technology, SE-100 44 Stockholm, Sweden. [b]System and Component Design, Department of Machine Design, KTH Royal Institute of Technology, SE-100 44 Stockholm, Sweden. [c]Department of Physics and Astronomy, Division of Materials Physics, Uppsala University, Uppsala, Sweden. Royal Institute of Technology, SE-100 44 Stockholm, Sweden. [d]Department of Electrical Energy, Metals, Mechanical Constructions and Systems, Ghent University, B-9052 Ghent, Belgium. [e]Surfaces, Processes and Formulation, RISE Research Institutes of Sweden, SE-100 44 Stockholm, Sweden.*

*[*]Correspondence: georgiap@kth.se*

*[†]Current address: Tokyo University of Science, Department of Mechanical Engineering, 6-3-1 Niijuku, Katsushika-ku, Tokyo 125-8585, Japan*

### Example neutron reflectivity of a gold electrode in air

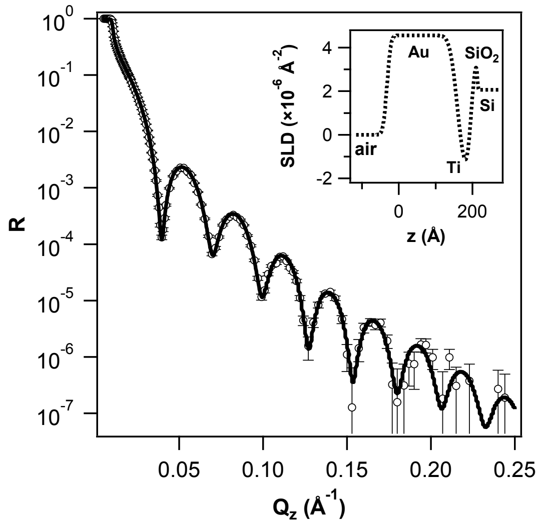


**Figure S1.** Example of the normalised reflectivity for a gold electrode in air. The symbols represent experimental data, while the solid line represents a fitted scattering length density (SLD) model fit to the data. The inset shows the corresponding SLD profile. This block was used for NR measurements in 20% [$P_{6,6,6,14}$][BMB] in PC.

**Table S1.** Example fitted parameters for a gold electrode in air corresponding to the model fit (solid line) presented in Fig. S1.

| Layer | SLD (×10$^{-6}$Å$^{-2}$) | Thickness (Å) | Roughness (Å) |
|---|---|---|---|
| Au | 4.56 | 190.0 | 8.35 |
| Ti | -1.91 | 37.2 | 15.9 |
| $SiO_2$ | 3.47 | 17.3 | 8.93 |
| Si | 2.07 | ∞ | 2.09 |

## Neutron reflectivity of pure PC

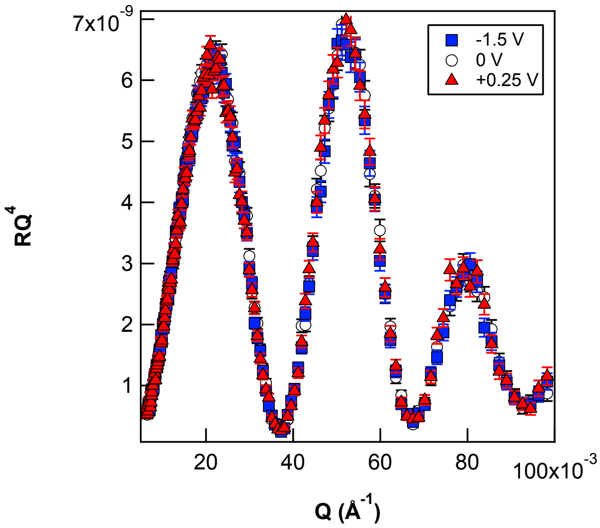


**Figure S2.** Neutron reflectivity of pure PC at a gold electrode for different applied potentials plotted as $RQ^4$ showing no electrochemical response. This data was collected on the reflectivity beamline INTER at the ISIS Facility, Rutherford Appleton Laboratory, UK.[44]

## SLD model parameters obtained from best-fits to NR measurements across IL solutions

**Table S2.** Fitted parameters for 5% w/w [$P_{6,6,6,14}$][BMB] in PC solution corresponding to the model fits (solid lines) presented in Fig. 2.

| Potential | SLD ($\times 10^{-6}$Å$^{-2}$) | Thickness (Å) | Gold/IL Roughness (Å) | IL/Bulk Roughness (Å) |
|---|---|---|---|---|
| 0 | 1.90 | 24.8 | 14.3 | 13.1 |
| -1.5 | 1.86 | 24.2 | 14.0 | 13.0 |
| +0.25 | 2.04 | 28.3 | 14.0 | 12.1 |

**Table S3.** Fitted parameters for 10% w/w [$P_{6,6,6,14}$][BMB] in PC solution corresponding to the model fits (solid lines) presented in Fig. 3.

| Potential | SLD ($\times 10^{-6}$Å$^{-2}$) | Thickness (Å) | Gold/IL Roughness (Å) | IL/Bulk Roughness (Å) |
|---|---|---|---|---|
| 0 | 2.94 | 23.8 | 15.5 | 7.49 |
| -1.5 | 2.34 | 22.2 | 13.3 | 6.97 |
| +0.25 | 2.68 | 26.8 | 13.6 | 14.2 |

**Table S4.** Fitted parameters for 20% w/w [$P_{6,6,6,14}$][BMB] in PC solution corresponding to the model fits (solid lines) presented in Fig. 4.

| Potential | SLD ($\times 10^{-6}$Å$^{-2}$) | Thickness (Å) | Gold/IL Roughness (Å) | IL/Bulk Roughness (Å) |
|---|---|---|---|---|
| 0 | 1.34 | 28.1 | 8.35 | 10.2 |
| -1.5 | 0.70 | 29.0 | 8.54 | 12.3 |
| +0.25 | 2.25 | 53.2 | 9.13 | 18.9 |

## Electrochemical Impedance Spectroscopy analysis

**(a)**

**(b)**

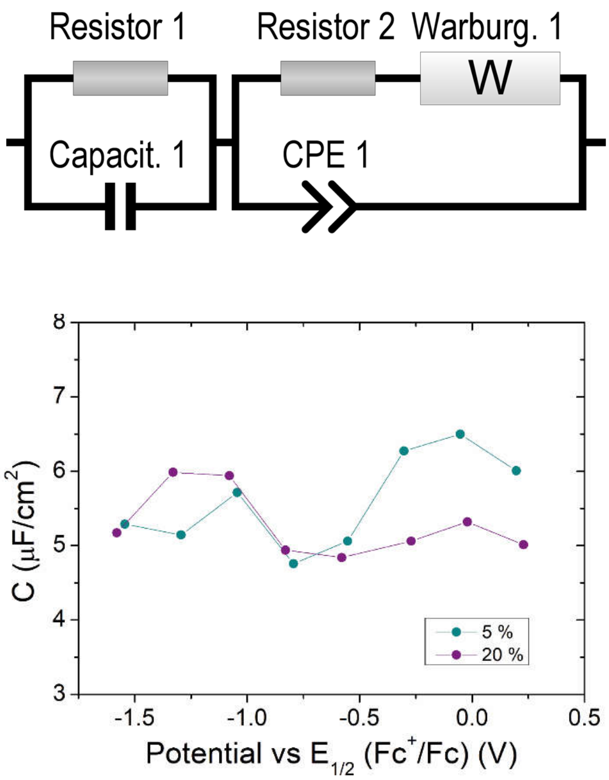


**Figure S3.** (a) Equivalent circuit used to model experimental EIS data. Resistor 1 represents contributions by cables, internal contact resistances inside the cell and the ion movement in the sample's bulk. Capacitor 1 accounts for the contributions by cables, stray capacitance due to the 3-electrode configuration and the bulk capacitance. The constant phase element 1 (= CPE 1) represents the differential interfacial capacitance of the sample/gold electrode interface, while resistor 2 and Warburg element 1 is related to diffusion processes at the interface. (b) Differential capacitance as a function of applied potential for solutions of 5 % and 20% [$P_{6,6,6,14}$][BMB] in PC on gold.

## Cyclic voltammetry

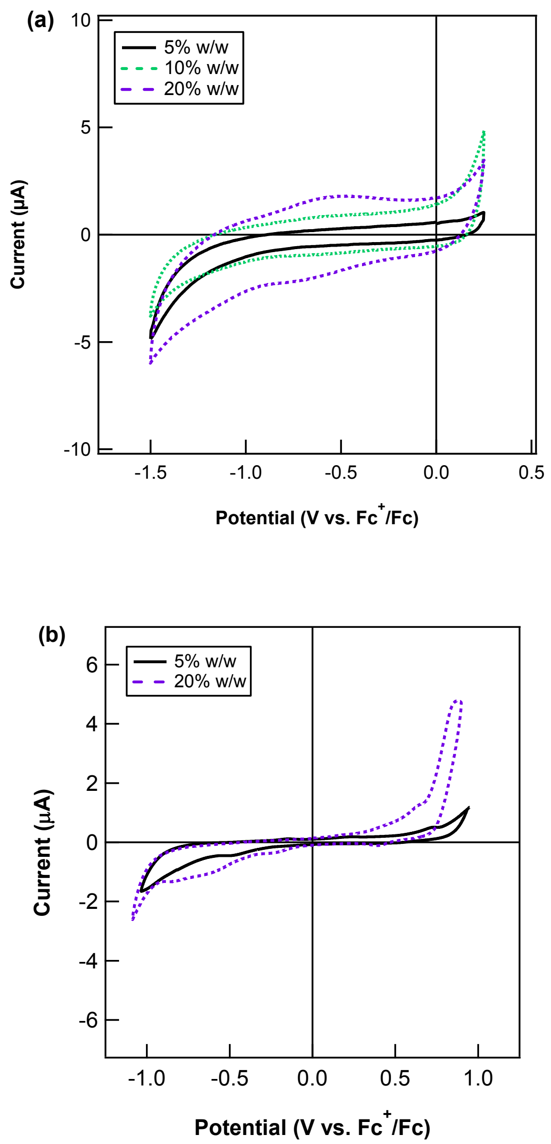


**Figure S4.** Representative cyclic voltammetry profiles for **(a)** solutions of 5, 10 and 20% w/w $[P_{6,6,6,14}]$[BMB] in PC performed in the electrochemical NR cell after performing neutron reflectivity measurements and **(b)** solutions of 5 and 20% w/w $[P_{6,6,6,14}]$[BMB] in PC in the electrochemical AFM cell. The potential is given with respect to $E_{1/2}$ $(Fc^+/Fc)$. The scan rate is 10 mV/s.

**IR measurements**

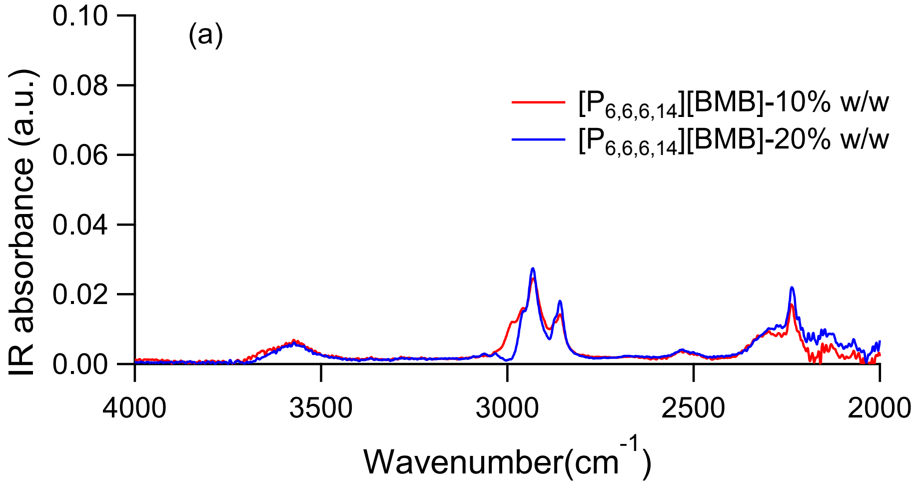


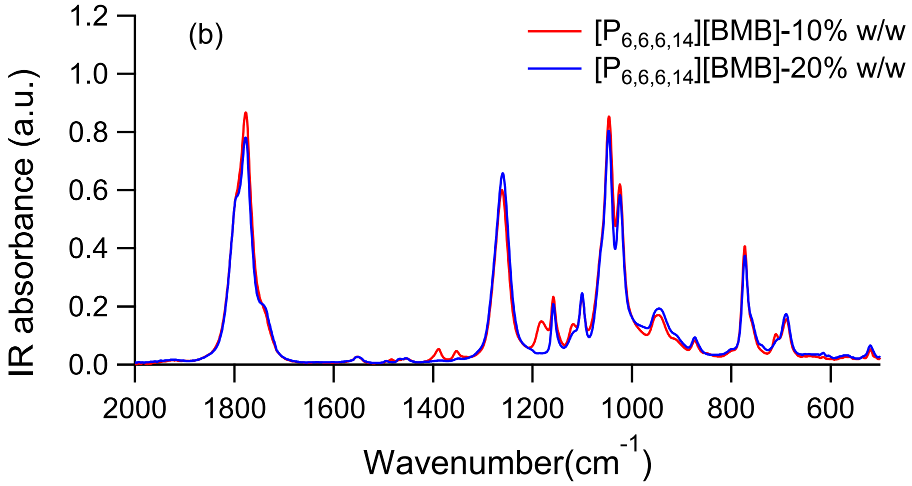


**Figure S5.** IR spectra of 10, 20% w/w $[P_{6,6,6,14}]$[BMB] in PC solutions in the wave range of (a) 4000 – 2000cm$^{-1}$ and (b) 2000 – 500 cm$^{-1}$. Water shows broad O-H stretching mode peaks with wave range of 3400 – 3700 cm$^{-1}$. Peaks at 3500 – 3650 cm$^{-1}$ are assigned to overtone peaks of C=O stretching by comparing with spectra of pure $[P_{6,6,6,14}]$[BMB] and PC.

## Current stabilisation during NR measurements

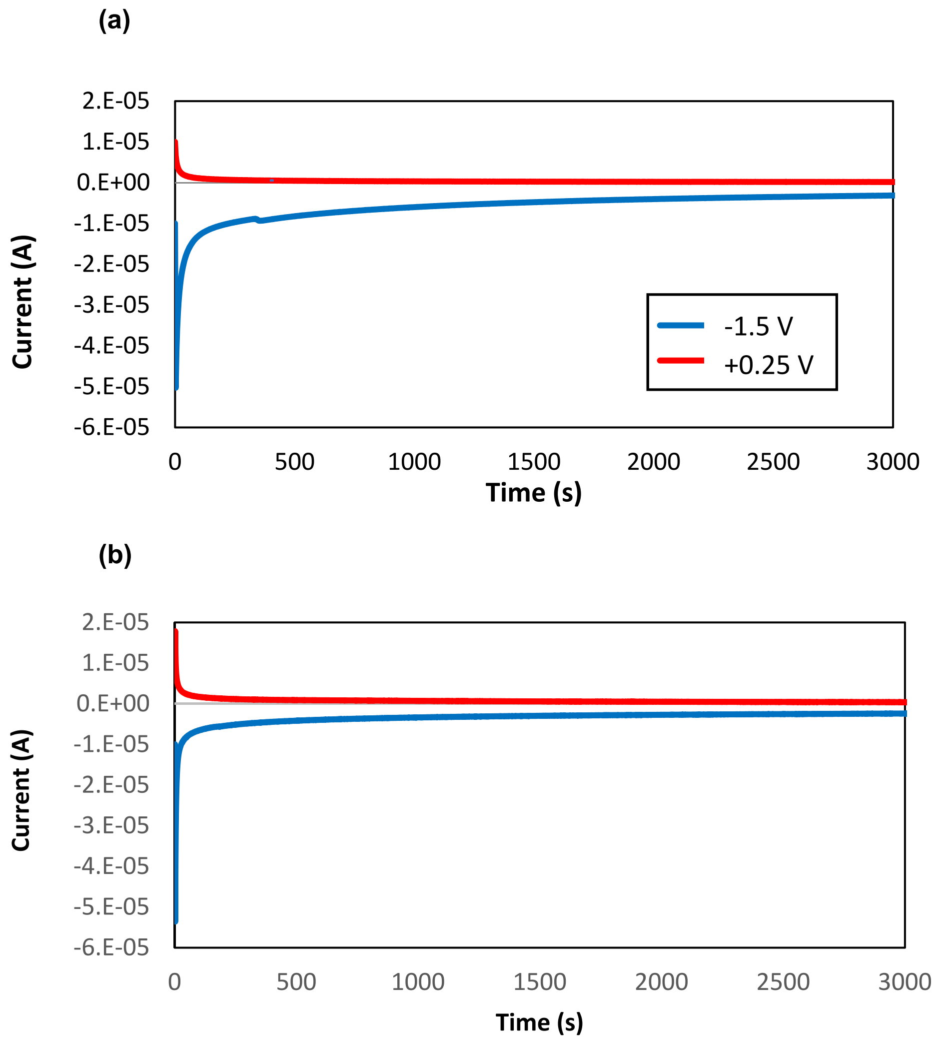


**Figure S6.** Current across the NR cell after application of different potentials plotted as a function of time for a **(a)** 5 and **(b)** 20% w/w solution of $[P_{6,6,6,14}]$[BMB] in PC. (Data for the 10% w/w solution is not presented due to a data saving error.)